PNAS
www.pnas.org

Supplementary Information for

Structural basis of Chikungunya virus inhibition by monoclonal antibodies

Qun Fei Zhou, Julie M. Fox, James T. Earnest, Thiam-Seng Ng, Arthur S. Kim, Guntur Fibriansah, Victor A. Kostyuchenko, Jian Shi, Bo Shu, Michael S. Diamond*, Shee-Mei Lok*

*Correspondence: Shee-Mei Lok (sheemei.lok@duke-nus.edu.sg); Michael S. Diamond (diamond@borcim.wustl.edu).

This PDF file includes:

www.pnas.org/cgi/doi/10.1073/pnas.2008051117

Material and Methods

Cells and virus

Vero (ATCC) cells were maintained at 37°C in Dulbecco's Modified Eagle medium (DMEM) supplemented with 10% fetal bovine serum (FBS). *Aedes albopictus* C6/36 cells (ATCC) were maintained in Roswell Park Memorial Institute (RPMI) 1640 media supplemented with 10% FBS at 29°C. CHIKV-East African strain and CHIKV-Ross strain were propagated in C6/36 cells growing in RPMI 1640 media supplemented with 2% FBS at 29°C. The CHIKV-La Reunion (LR) OPY-1 strain was a gift from S. Higgs (Kansas State University) and was initially produced from an infectious cDNA clone then passaged in C6/36 cells grown in Leibovitz (L-15) media supplemented with 10% heat-inactivated FBS, 100 U/ml penicillin and streptomycin, 10mM HEPES, 1x non-essential amino acids, and 1mM sodium pyruvate at 28°C. The virus titer was determined by plaque assay or focus forming assay as described previously (1, 2). Before our acquisition, CHIKV-East African and CHIKV-Ross were passaged five times and four times, respectively in C6/36 cells.

Monoclonal antibody CHK-263 and CHK-124 production and digestion

The mouse MAbs CHK-263 and CHK-124 were described previously (1). After production by the hybridoma cell lines, the antibodies were purified through High Trap Protein G column (GE Healthcare) and S200 increase size-exclusion chromatography (GE Healthcare). Purified antibodies were digested by papain (Thermo Fisher Scientific) to produce the Fab fragments according to the manufacturer's instruction. Briefly, the purified IgG in digestion buffer (20 mM sodium phosphate, 10 mM EDTA, 2 nM Cysteine-HCl) was incubated at 37°C for 2 h with immobilized papain at 37°C. After

digestion, the Fab fragment was purified by anion exchange (resource Q, GE Healthcare) and gel filtration (Superdex 200 increase 10/300 GL, GE Healthcare) chromatography.

Plaque reduction neutralization test

The neutralizing activity of the antibodies against CHIKV was evaluated by a plaque reduction neutralization test (PRNT) (1). Vero cells ($5x10^5$ cells/well) were plated in 24-well plates (Thermo fisher scientific) for 24 h. Two-fold serial dilutions of CHK-263 and CHK-124 were prepared and incubated at 37°C for 1 h with an equal volume of CHIKV diluted to 2 $x10^3$ PFU/mL respectively. A total of 100 µl of each mixture was added to Vero cell monolayers in a 24-well plate and incubated at 37°C for 1.5 h. The infected cells were washed with DMEM medium with 2% FBS to remove the unbound CHIKV:antibody complex, overlaid with carboxyl-methyl cellulose and incubated at 37°C for 48 h. Cells were fixed with 25% formaldehyde and stained using 0.5% crystal violet, and the plaques were counted. Relative infection was calculated by comparing the number of plaques to the wells infected with CHIKV in the absence of antibody. The $PRNT_{50}$ value was determined as the concentration of the antibody that causes a 50% reduction in the plaque numbers.

Mouse studies

Experiments were performed in accordance with the recommendations in the *Guide for the Care and Use of Laboratory Animals* of the National Institutes of Health after approval by the Institutional Animal Care and Use Committee at the Washington University School of Medicine (assurance number: A3381-01). All infections were performed under anaesthesia with ketamine hydrochloride (80 mg/kg) and xylazine (15 mg/kg).

***In vivo* experiments**

Four-week-old male C57BL/6 mice were obtained from Jackson Laboratories. FcRγ$^{-/-}$ mice were obtained from Taconic, backcrossed using speed congenic analysis onto a C57BL/6J background, and bred at the Washington University Animal Facility. CHK-124, CHK-263, or an isotype control (WNV E60) (3) was administered by intraperitoneal injection one day prior to subcutaneous inoculation in the left rear footpad with 10^3 FFU of CHIKV-LR in Hank's Balanced Salt Solution (HBSS) supplemented with 1% heat-inactivated-FBS. Ipsilateral foot swelling was measured using digital calipers (width x height) at 3 dpi and normalized to measurements taken prior to infection. At 3 dpi, tissues were collected following perfusion with PBS. Viral burden was determined using qRT-PCR using RNA isolated from viral stocks as a standard to determined FFU equivalents, as previously described (4). Briefly, tissues were homogenized in DMEM supplemented with 2% heat-inactivated FBS, 10mM HEPES, and 100 U/ml penicillin and streptomycin using a MagNA Lyser (Roche). RNA was isolated from clarified homogenate using the RNeasy mini kit (Qiagen) or MagMax-96 viral RNA isolation kit (Applied Biosystems) with the Kingfisher Flex purification system (Thermo) and qRT-PCR was performed using the RNA-to-Ct one-step kit (Applied Biosystems) with E1 specific primers/probe.

Pre- and postattachment neutralization assays

The pre- and postattachment neutralization assays were conducted as previously described (1, 5). Briefly, Vero cells were grown in 24-well plates for 24 h and then chilled for 15 min at 4°C. For the preattachment assay, two-fold dilutions of the IgG or Fab of CHK-124 and CHK-263 starting with a concentration of 8 μg/mL (IgG) or 16 μg/mL (Fab) were prepared. The CHIKV stock was diluted to 10^3 PFU/mL and mixed

with the same volume of the antibody. After an incubation at 4°C for 1 h, 200 µl/well of the mixture was added to the Vero cell monolayers in the 24-well plate and incubated at 4°C for 1 h. Subsequently, the infected cell monolayers were washed two times with cold medium and incubated at 37°C for 15 min to allow virus internalization. The cells were overlaid with carboxyl-methyl cellulose and incubated at 37°C for 48 h before fixing and staining. For the postattachment assay, the CHIKV stock was diluted to 10^3 PFU/mL. A total of 200 µl/well of the CHIKV sample was added to the Vero cell monolayers in the 24-well plate and incubated at 4°C for 1 h. The cell monolayers were washed two times to remove free virus before incubation with the serially diluted antibody at 4°C for 1 h. Subsequently, the infected cells were washed two times, incubated at 37°C for 15 min and then overlaid with carboxyl-methyl cellulose. After incubation at 37°C for 48 h, the cell monolayers were fixed and stained.

RT-qPCR quantification of the virus on the cell surface

5×10^4 PFU of CHIKV-East African was incubated with the IgG or Fab at 4°C for 1 h before adding to the prechilled Vero cells. After incubation at 4°C for 1 h, the cell monolayers were washed twice to remove unbound virus. The cells were lysed and total RNA was purified using RNeasy mini kit (Qiagen). Complementary DNA was synthesized using qScript cDNA SuperMix (Quantabio). Real-time quantitative PCR (qPCR) was performed using iQ™ SYBR Green supermix kit (Bio-Rad) in a CFX 96 Real-Time System (Bio-Rad). Glyceraldehyde-3-phosphate dehydrogenase (GAPDH) was used as the housekeeping gene to normalize samples. Gene-specific primers were used in RT-qPCR to quantify the amount of viral RNA. Results were normalized as the percentage to the value of control group (no MAb treatment).

CHIKV-SP-Fwd: 5' ACGCTTCGAAGTTCACCCAT;

CHIKV-qPCR-Rev: 5' GCTGTACGGGCTCCTTCATT;

Vero-GAPDH-Fwd: 5'-GAACGGGAAGCTTGTCATCAATGG-3';

Vero-GAPDH-Rev: 5'-TGTGGTCATGAGTCCTTCCACGAT-3'.

Mxra8 blocking experiment

Maxisorp ELISA plates were coated with anti-CHIKV mAbs CHK-152 and CHK-166 (2 µg/ml) (1) overnight in sodium bicarbonate buffer, pH 9.3 Plates were washed four time with PBS and blocked with 4% BSA for 1 h at 25ºC. CHIKV VLPs (1 µg/ml) (6) were diluted and added for 1 h at 25ºC. After washing, CHIKV mAbs (CHK-124 and CHK-263) or Mxra8 mouse-Fc fusion protein (all at 10 µg/ml) were incubated for 30 min. Subsequently, without washing, serially diluted Mxra8 human-Fc fusion protein was added for 1 h at 25ºC. Plates were washed with PBS and incubated with horseradish peroxidase conjugated goat anti-human IgG (1:5000 dilution, Jackson Immunoresearch) for 1 h at 25ºC. After washing, plates were developed with 3,3'-5,5' tetramethylbenzidine substrate (Thermo Fisher) and 2N H_2SO_4. Plates were read at 450 nM using a TriStar Microplate Reader (Berthold).

Liposome preparation

Liposomes were prepared from the following lipid mixture: 1,2-dioleoyl-sn-glycero-3-phosphocholine (DOPC): 1,2-Dioleoyl-sn-glycero-3-phosphoethanolamine (DOPE): Sphingomyelin (SPM): Cholesterol (Chol) in a molar ratio of 1/1/1/1.5. The method to prepare the 100 nm unilamellar liposomes has been described previously (7). Briefly, the lipid mixtures dissolved in benzene/methanol (95:5) were dried under vacuum overnight and then resuspended in NTE buffer by vigorous vertexing in 60°C, followed by five freeze-thaw cycles by altering immersion into liquid nitrogen and 37°C water

bath. Finally, we extruded the lipid suspension 50 times through double-stacked track-etched 100 nm-pore polycarbonate filters (GE Osmonics) using a LIPEX extruder. Liposome size was validated using dynamic light scattering.

DiD-labelling of CHIKV particles

The purified CHIKV-East African particles were labelled with a self-quenching concentration of DiD, a fluorescent lipid. A total of 50 µl of a 1 mM DiD solution from a Vybrant cell-labelling kit (Molecular Probes, Eugene, OR) was injected into 1.5 mL of diluted purified virus (E2 final concentration: ~30 ug/ml) while vortexing. The mixture was incubated for 30 min at 37°C. To remove the free dye, the mixture was passed through a PD-10 column (GE Healthcare) preequilibrated using NTE buffer. Fractions were collected, and the fluorescence in different fractions was measured using Tecan microplate reader with an emission wavelengths of 665 nm. The labelled virus was stored at 4°C and used within 3 days.

DiD-labelled virus fusion assay

DiD-labelled virus was incubated with an equal volume of IgG or Fab (or medium) at 37°C for 30 min. For the negative control group without antibody, NTE buffer was used to top up the volume. For the fusion-inhibition-positive control, DEPC at a final concentration of 17 mM was added to the diluted virus. After incubation, the virus-antibody complex and the control groups were mixed with an equal volume of liposomes at a concentration of 75 µM in 2% BSA assay buffer. The fusion reaction was initiated as the pH of the solution was adjusted to pH 5.5 by adding a pre-titrated amount of MES/acetic acid buffer. After shaking the plate for 30 s and equilibrating 5 min at 37°C, the fluorescence was recorded at excitation and emission wavelengths of

633nm (slit width 9) and 665 nm (slit width 20) respectively, using a Tecan microplate reader. At the end of each recording, Triton X-100 was added to a final concentration of 0.1% to unquench the DiD in the samples ("100% lipid mixing"). The extent of fusion was calculated as the percentage of the fluorescence emission before adding Triton X-100 to the fluorescence after adding Triton X-100.

Virus egress assay

Vero cells in 24-well plates were inoculated with CHIKV-East African at an MOI of 10. After 1 h at 37^{o}C, cells were washed 6 times with medium. The cells were incubated with 200 µl of medium containing dilutions of the indicated IgG or Fab at 37^{o}C. The cell supernatant was collected at 1 h and 6 h after adding antibodies and treated with 50 µg/ml RNase A (Qiagen). RNA was isolated from the supernatant using an RNAeasy Mini kit, and CHIKV RNA was measured using RT-qPCR. The amount of viral RNA was compared with a viral stock of known titer to determine PFU equivalents/ml.

Measurement of the virus aggregation by dynamic light scattering

CHIKV-East African virus was purified and diluted in NTE buffer to a concentration of 0.2 mg/ml E2 protein (concentration estimated by SDS-PAGE with BSA as a standard). Equal volume of antibodies were mixed with the virus at the IgG:virion molar ratios ranging from 1:1 to 1200:1, and incubated at 37°C for 30 min. The sizes of immune complex were measured by dynamic light scattering (DLS) at 25°C using the Zetasizer Nano S machine (Malvern). Each sample was measured twelve times, and the result was analysed using Zetasizer Nano software version 6.01. The size of the immune complex was determined as intensity weighted mean hydrodynamic size. The change of the hydrodynamic size compared to the size of virion alone was calculated.

For the same sample, infectivity of the complexed virus was determined using a standard plaque assay in Vero cells. Neutralization index was determined as the log reduction of the infectious virus (PFU/ml) in the immune complex compared to the virus alone.

Biolayer interferometry (BLI) assay

The binding kinetics of CHK-124 Fab and CHK-263 Fab to CHIKV-East African were monitored in real-time at 25°C using a ForteBio Octet Red96 device (Pall ForteBio). Anti-CHIKV antibody E26D9.02 (Novus Biologicals) at a concentration of 50 µg/mL in PBS was loaded on the anti-hIgG Fc capture (AHC) biosensors (Pall ForteBio). After a brief rinse, these biosensors captured the CHIKV particles with the E2 protein concentration of 50 µg/mL in NTE buffer (10 mM Tris-HCl pH 8.0, 120 mM NaCl and 1 mM EDTA) followed by 5-minute buffer exchange and stabilization in PBS buffer. The CHK-124 Fab and CHK-263 Fab were prepared as a two-fold serial dilution starting at 500 nM (25 µg/mL). Association of CHIKV particles with the Fab molecules was measured for 120 s followed by a 120-second dissociation in PBS buffer. The binding kinetics were analysed using a standard 1:1 binding model under the Octet Data Analysis v10.0.1.6 software (Pall ForteBio).

Virus sample preparation

C6/36 cells were grown to ~90% confluency before inoculation with CHIKV-East African or CHIKV-Ross strain at a multiplicity of infection (MOI) of 10 and incubation at 29°C for 48 h. The virus-containing media was clarified by centrifugation at 8,000×*g* for 30 min. The virus was precipitated overnight from the supernatant using 8% (w/v) polyethylene glycol (PEG) 8000, and resuspended in NTE buffer (10 mM Tris-HCl pH

8.0, 120 mM NaCl and 1 mM EDTA). The suspension was centrifuged at 8,000 × *g* for 30 min, and the resulting pellet containing the virus was resuspended in NTE buffer and purified by ultracentrifuges through a 24% (w/v) sucrose cushion at 75,000×*g* for 90 min followed by a linear 10-30% w/v potassium tartrate gradient with 30% (w/v) glycerol at 126,000×*g* for 2 h. The virus band, visualized by its light scattering ability, was extracted and buffer exchanged into NTE buffer. Finally, the purified virus was concentrated using a concentrator with 100-kDa molecular weight cut-off filter. All steps of the purification procedure were performed at 4°C.

Sample preparation for Cryo-electron microscopy

CHIKV virus samples were mixed with the CHK-263 Fab or CHK-124 Fab at a molar ratio of 1.5 Fab to every E2 protein and incubated at 37°C for 30 min, then kept at 4°C before freezing on cryo-EM grids. About 2 µl of the sample was applied to a precooled cryo-EM grid with lacey carbon covered with thin carbon film. The grid was then blotted with filter paper at 4°C with 100% humidity for 1-2 s, and flash-frozen in liquid ethane by using the Vitrobot Mark IV plunger (FEI, The Netherlands).

Data collection and image processing

The images of the frozen CHIKV-Ross:CHK-124 Fab complex, CHIKV-East African:CHK-263 Fab complex and CHIKV-East African:CHK-263 IgG complex were taken with the FEI Titan Krios electron microscope at 300 keV with a nominal magnification of 47,000x and a FEI Falcon II direct electron detector. Images were collected using Leginon (8) in movie mode, with a total exposure of 2 s and a total dose of ~20 $e^{-}/Å^2$. The frames from each 'movie' were aligned using MotionCorr (9) to produce full-dose images used for particle selection and orientation search, and the

images from the first several frames amounting to the dose of about 20 $e^{-}/Å^2$ was used in 3D reconstruction. The images were taken at a defocus range of 0.5~2.5 μm. cisTEM (10) and Gctf (11) were used to estimate the astigmatic defocus parameters. Particle picking was undertaken using cisTEM. Orientation search and three-dimensional reconstruction of the picked particles were performed using cisTEM and RELION (12, 13). Briefly, 5,777, 3,851, and 2780 micrographs were collected for the CHIKV:CHK-124 Fab complex, CHIKV:CHK-263 Fab complex, and CHIKV:CHK-263 IgG, respectively. After automatically particle picking using cisTEM, a total number of 116,021, 176,396, and 45,657 particles were selected for further reconstruction of CHIKV:CHK-124 Fab complex, CHIKV:CHK-263 Fab complex and CHIKV:CHK-263 IgG, respectively. The two-dimensional classification was performed in cisTEM, where broken and non-viral particles were discarded. The three-dimensional classification was performed in cisTEM to improve the homogeneity of the sample. Initial models generated using cisTEM were used as the references for the reconstruction. Following this, 68,406 particles for the CHIKV:CHK-124 Fab complex, 164,158 particles for the CHIKV:CHK-263 Fab complex, and 29,946 particles for the CHIKV:CHK-263 IgG complex were selected to generate the final map using cisTEM. The final resolution of the structures of CHIKV:CHK-124 Fab complex, CHIKV:CHK-263 Fab complex, and CHIKV:CHK-263 IgG complex were determined to 5.2-, 4.7- and 5.9-Å respectively, using RELION with a Fourier shell correlation (FSC) cutoff of 0.143. Localized reconstruction (14) was performed to overcome the flexibility among the sub-regions and improve the resolution of the sub-regions of the complex structures. A Sub-box of 342 Å in length which includes five trimeric spikes at the 5-fold vertices and sub-box with the same length including four trimeric spikes at the 3-fold vertices were applied to the CHIKV:CHK-124 Fab complex structure. The density of the sub-

regions was extracted and refined using RELION. The final resolution of the sub-particles was determined by the gold standard FSC of 0.143 in FSC using RELION. The 5-fold, and 3-fold sub-particles of the CHIKV:CHK-124 Fab complex were determined to a resolution of 4.9-Å and 4.8-Å respectively. For the CHIKV:CHK-263 Fab complex, a sub-box of 321 Å in length was applied to the 5-fold, 3-fold, and 2-fold vertices respectively to refine the density of sub-particles in the corresponding regions. The sub-particles at the 5-fold vertices were classified into five classes. Each class has two Fab binding at different trimeric spikes. We applied symmetry expansion (13, 15) to the 5-fold sub-particles and combined particles with the same conformation for further refinement. Finally, the sub-particles around the 5-fold, 2-fold and 3-fold vertices of the CHIKV:CHK-263 Fab complex were determined to a resolution of 4.5-, 4.1-, and 4.4-Å, respectively. For the CHIKV:CHK-263 IgG complex, a sub-box of 496 Å in length was applied to the 5-fold and 2-fold vertices respectively to refine the density of sub-particles in the corresponding regions, and the sub-regions around the 2-fold vertex were determined to 9.4-Å resolution.

Protein structure building

Based on their sequence, we used the Swiss Model website to generate the protein model of the CHK-124 Fab heavy chain and light chain (PDB code: 5FXC and 6BPC respectively), CHK-263 Fab heavy chain and light chain (PDB code: 3ETB and 5VJQ respectively), and CHIKV E1 protein (PDB code: 6NK5), E2 protein (PDB code: 6NK5) and capsid proteins (PDB code: 6NK5). The protein models were fitted into the cryo-EM map first as rigid bodies in Chimera. For the CHIKV:CHK-263 Fab complex structure, PHENIX real-space refinement (16) was performed for further model fitting

and refinement with secondary structure restrain, followed by manual structure building using COOT (17). The quality of the model fitting was validated by Molprobity (18).

Electrostatic potential calculations

Electrostatic potentials of protein surfaces were calculated using Adaptive Poisson-Boltzmann Solver (APBS) (19) and PDB2PQR (20) packages. The structures of the E1-E2 heterodimer and the Fab molecules from the CHIKV:Fab complex structures were processed with the PDB2PQR web server (nbcr-222.ucsd.edu/pdb2pqr_2.0.0/) to prepare the PDB files for APBS. A PARSE force field (21) was applied and PROPKA (v3.0) (22) was used to assign pKa values. APBS was then used to calculate the electrostatic properties of the protein surface.

Statistical analysis

Statistical significance was determined using GraphPad Prism version 8.2 (La Jolla, CA) and assigned with P values < 0.05. The statistical test used for each graph is indicated in the Figure legend. Briefly, for foot swelling analysis, significance was determined using a one-way ANOVA with a Tukey's post-test. For virological studies, a Kruskal-Wallis test with a Dunn's post-test was used to determine significance.

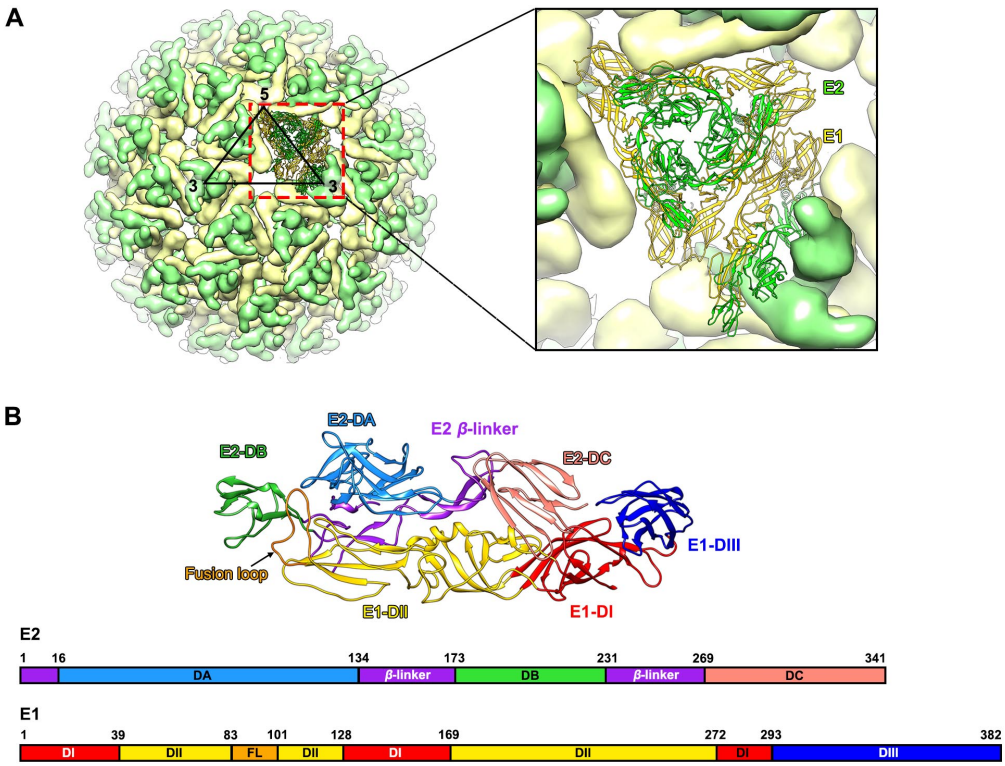

Fig. S1. Structure of CHIKV E1 and E2 surface envelope proteins. (*A*) The surface proteins E1-E2 heterodimer is organized in a *T=4* icosahedral symmetry with four E1-E2 heterodimers (shown in ribbons) in an asymmetric unit. The whole virus surface of CHIKV virion consists of 80 trimeric spikes. The E1 and E2 proteins are colored as yellow and green, respectively. (***B***) Both E1 and E2 proteins ectodomains contains three domains. On E1: E1-DI (red), E1-DII (yellow), E1-DIII (blue); and on E2: E2-DA (light blue); E2-DB (green); E2-DC (salmon). Fusion loop in E1-DII is colored in orange, and the E2 *β*-linker is in purple. The numbers on the linear diagrams in bottom panel indicate the amino acid regions that form the domains.

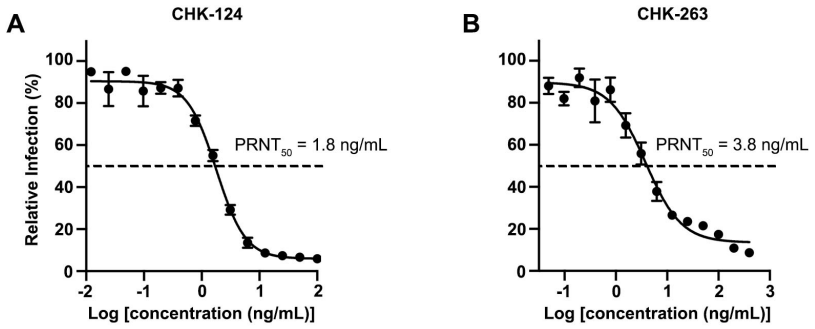

Fig. S2. CHK-124 and CHK-263 potently neutralize CHIKV infection. (***A*** and ***B***) Plaque reduction neutralization tests (PRNT) shows that CHK-124 (***A***) and CHK-263 (***B***) neutralize CHIKV in the nanogram/mL range. The antibodies were incubated with CHIKV particles before the CHIKV:antibody mixture was added to Vero cells and incubated for 48 h for plaque formation. Relative infection was determined by comparing the wells treated with antibody with wells without antibody treatment. $PRNT_{50}$ values were determined by non-linear regression using GraphPad Prism v8.0. Data are presented as mean ± SEM from at least three independent experiments.

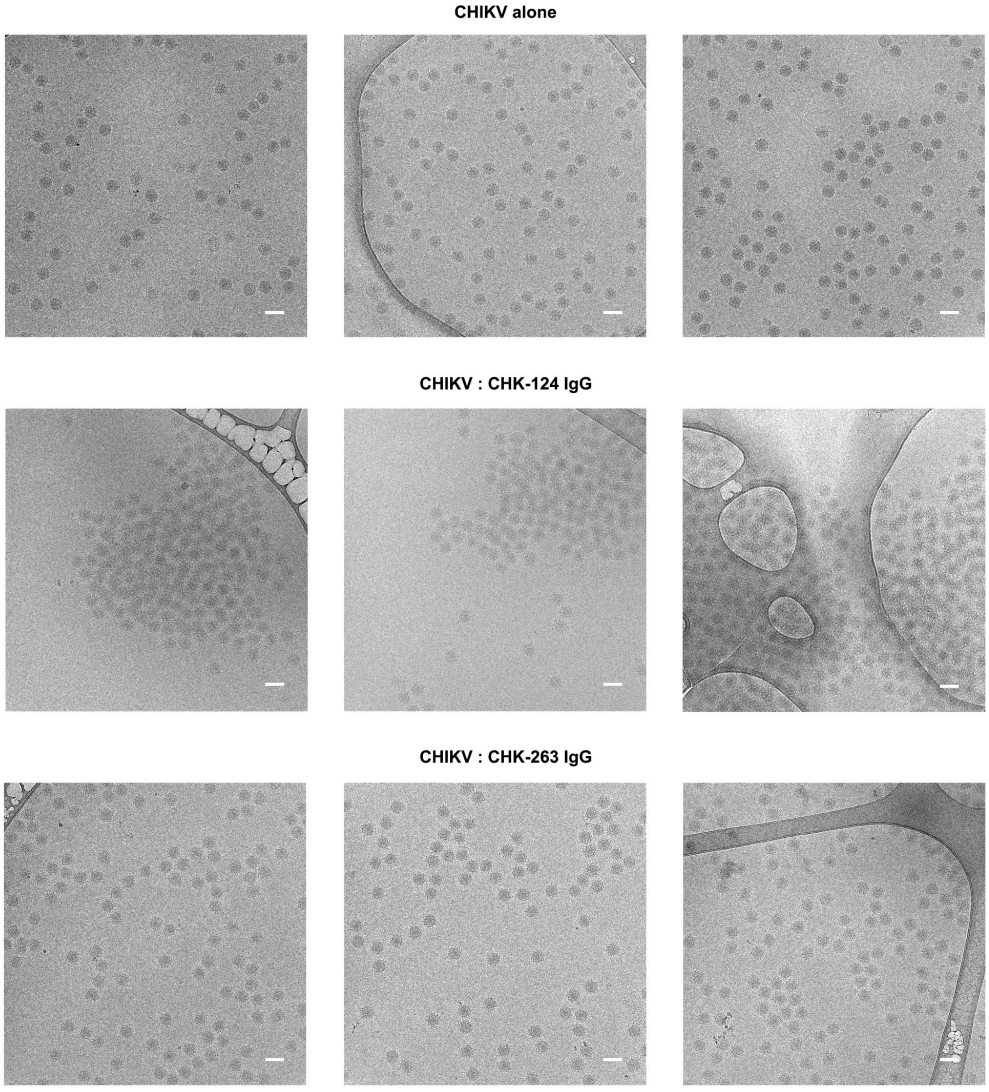

Fig. S3. Cryo-EM micrographs of CHIKV particles complexed with CHK-124 or CHK-263 IgGs at a E2: IgG molar ratio of 1:1.5. Results shows that at saturating IgG concentration CHK-124 aggregates virus particles whereas CHK-263 does not. Micrographs showing uncomplexed CHIKV (***top***), CHIKV complexed with CHK-124 IgG (***middle***), and CHIKV complexed with CHK-263 IgG (***bottom***). (Scale bar: 1000 Å.)

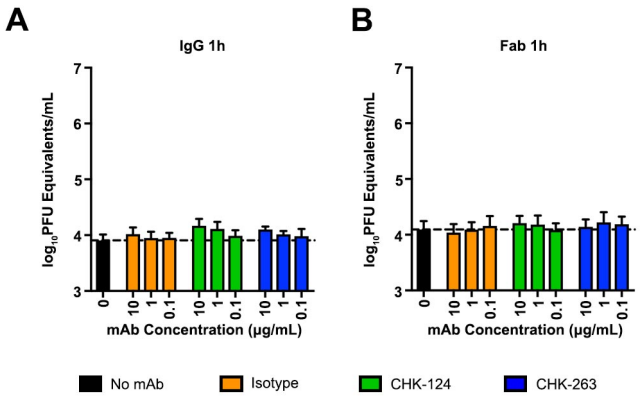

Fig. S4. CHK-124 and CHK-263 have no inhibitory effect on viral egress at one hour post-infection. (***A***-***B***) Vero cells were infected with CHIKV for 1 h at 37°C. Following extensive washing of input virus, medium was added with the indicated concentrations of IgG (***A***) or Fab (***B***) of CHK-124, CHK-263, or an isotype control. Viral RNA in the supernatant was quantified by qRT-PCR at 1 h after adding antibodies. Data are the mean ± SEM from three independent experiments. Significance was determined by one-way ANOVA with Dunnett's post-test compared to isotype control.

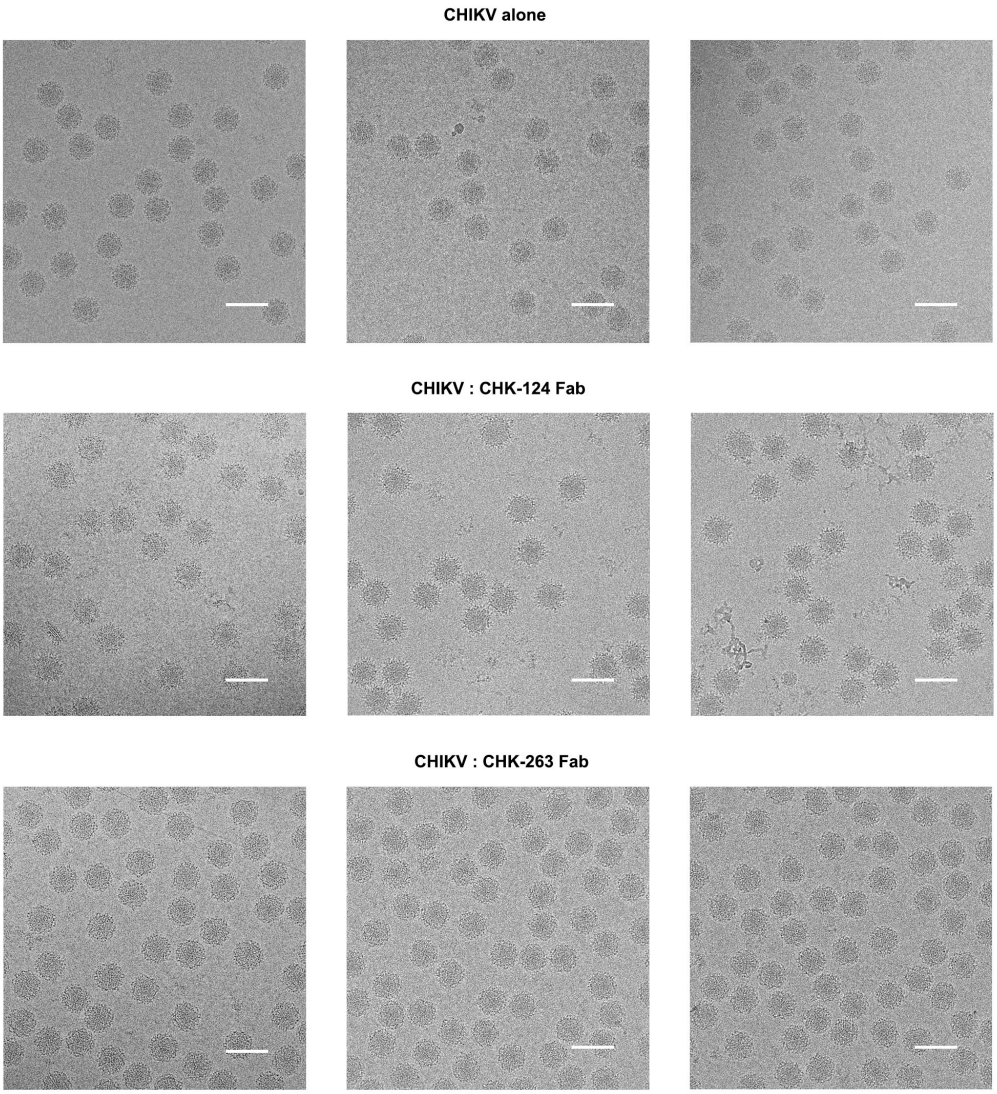

Fig. S5. Cryo-EM micrographs of CHIKV particles complexed with CHK-124 or CHK-263 Fabs at a E2: IgG molar ratio of 1:1.5. (***A-C***) Micrographs showing uncomplexed CHIKV (***top***), CHIKV complexed with CHK-124 Fab (***middle***), and CHIKV complexed with CHK-263 Fab (***bottom***). (Scale bar: 1000 Å.)

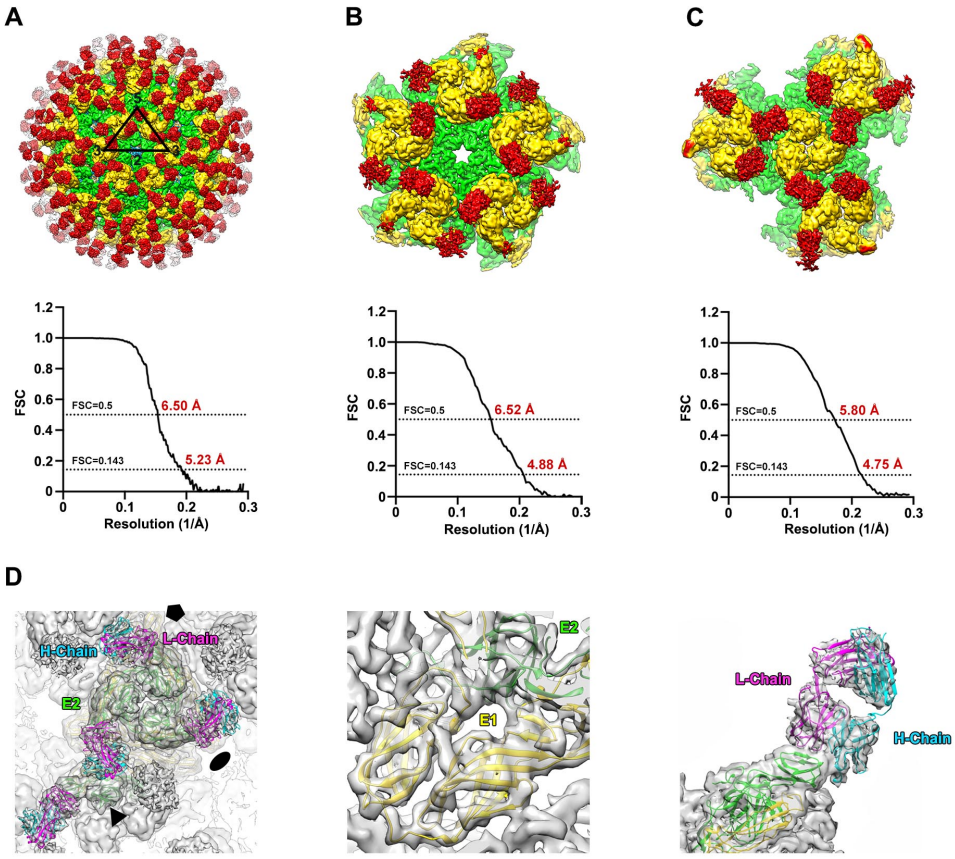

Fig. S6. Cryo-EM density maps and protein model fitting of CHIKV:CHK-124 Fab complex structure. (***A-C***) The cryo-EM map of the complexed particle was determined to 5.2-Å (***A***). Localized reconstructions of sub-regions around 5-fold (***B***), and 3-fold (***C***) vertices of CHIKV:CHK-124 Fab complex were determined to 4.9- and 4.8-Å resolution, respectively. The bottom panels showed FSC with the cut-off at 0.5 and 0.143. (***D***) The fit of the cryo-EM structures E1, E2 and homology model of CHK-124 Fab into the cryo-EM density map showed that the CHK-124 Fab binds perpendicularly with respect to the CHIKV lipid envelope surface, and its binding did not change the overall CHIKV virus surface structure. Density is shown as grey transparent surfaces. An asymmetric unit of the fitted four E1:E2 heterodimers and CHK-124 Fab molecules are shown as ribbons. E1 and E2 are colored in yellow and green, respectively. The Fab light and heavy chains are colored in magenta and cyan, respectively.

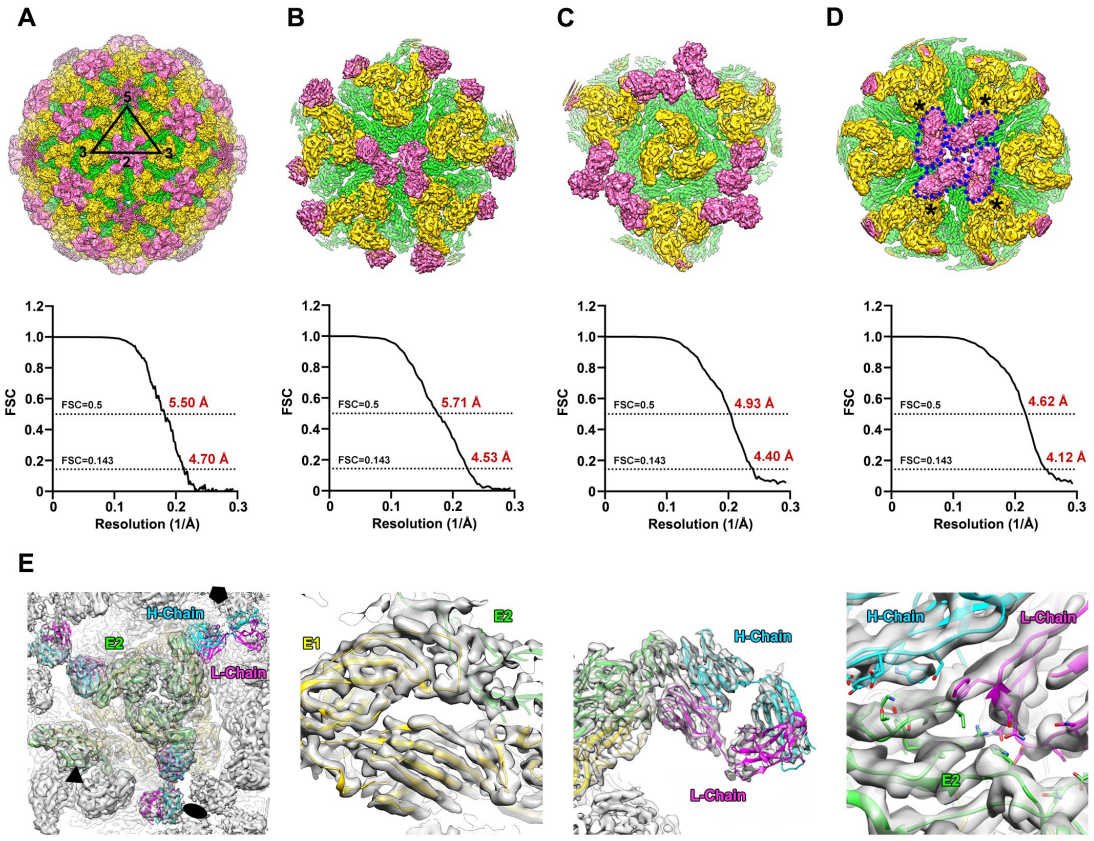

Fig. S7. Cryo-EM density maps and protein model fitting of CHIKV:CHK-263 Fab complex structure. (***A-D***) The cryo-EM structure of the complexed particle was determined to 4.7-Å (***A***). Localized reconstructions of the sub-region around 5-fold (***B***), 3-fold (***C***) and 2-fold (***D***) vertex of the CHIKV:CHK-1263 Fab complex. These maps were determined to 4.1- to 4.5-Å resolutions. The Fabs at the 2-fold vertex are indicated by blue dotted circle. The E1-E2 bound by the Fabs were labelled by an asterisk (*). (***E***) The fit of the cryo-EM structures of E1, E2 and the homology model of CHK-263 Fab into the cryo-EM density map showed that the CHK-263 Fab binds laterally on the CHIKV surface, and its binding also did not change the overall structure of the CHIKV envelope proteins. There are however, only three out of four E1-E2 heterodimers being bound by the Fabs within an asymmetric unit. The light and heavy chains of CHK-263 Fab are colored in magenta and cyan, respectively.

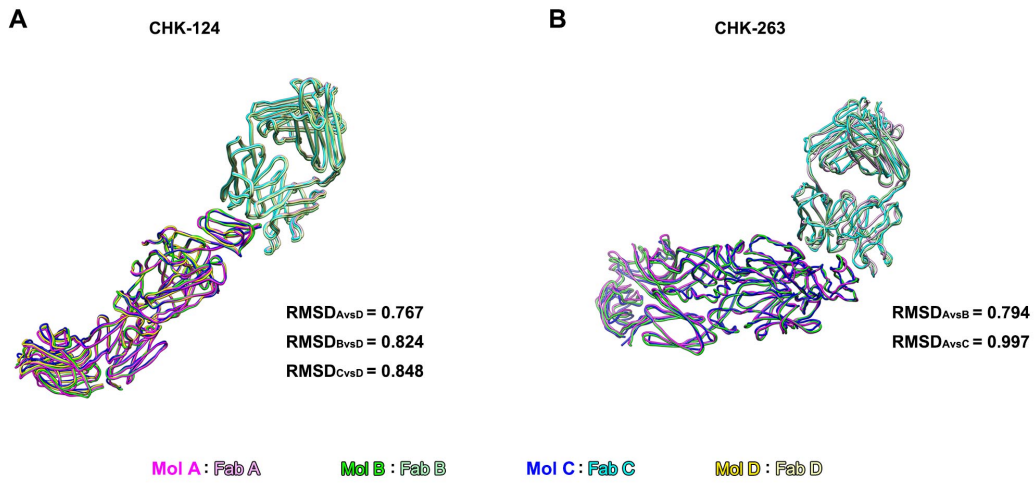

Fig. S8. **Superpositions of the individual bound E1-E2:Fab complexes within an asymmetric unit and their RMSD.** The RMSD of the two superimposed structures were calculated using the Matchmaker tool of Chimera. The four individual E1-E2 heterodimers within an asymmetric unit are molecules A, B, C and D, as indicated in **Fig. 3**

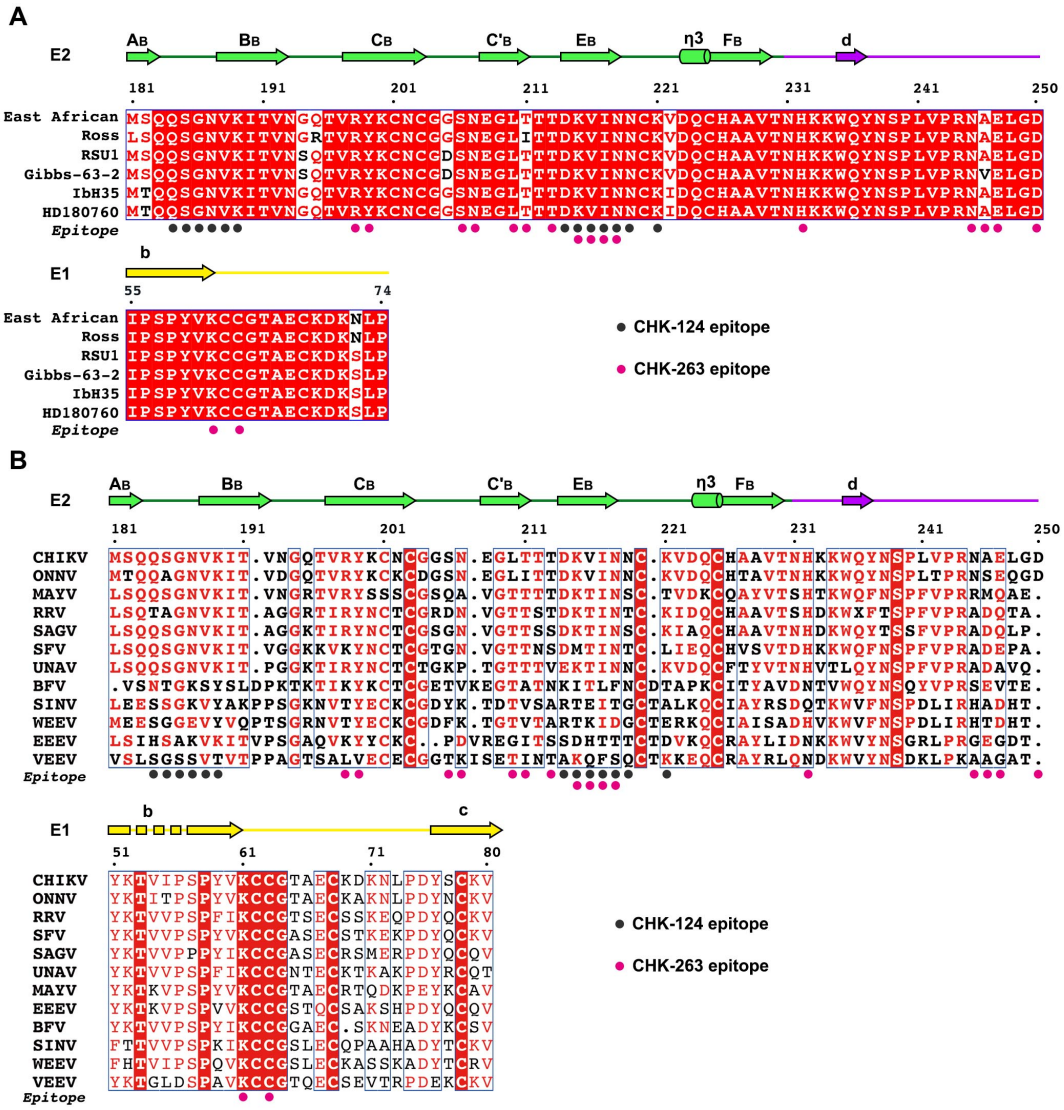

Fig. S9. Sequence alignment of the epitope of CHK-124 and CHK-263 in different alphaviruses. (*A*) Sequence alignment of the epitope region of six CHIKV strains. Strands are labelled above the amino acid sequence. The aligned strains represent three CHIKV genotypes (East African and Ross: East, Central, and South African (ECSA); RSU1 and Gibbs-63-2: Asian; IbH35 and HD180760: West African). (***B***) Sequence alignment between 12 representative alphaviruses showed that the epitope of CHK-124 is highly conserved among Chikungunya virus (CHIKV), O'nyong'nyong virus (ONNV), Mayaro virus (MAYV), Ross River virus (RRV), Sagiyama virus (SAGV), Semliki Forest virus (SFV) and Una virus (UNAV), and the epitope of CHK-263 in E1 protein is identical across all alphaviruses whereas the CHK-263 epitope in E2 protein is only moderately conserved. The residues on the envelope proteins that interact with CHK-124 and CHK-263 are labelled as dark grey dots and pink dots, respectively, in the bottom row. A red background with white font highlights identical residues across alphaviruses. Red fonts in a white background indicate similar residues. Secondary structures are shown above the corresponding amino acid sequence (23). The colors of these secondary structures indicate the domains of E1 and E2 (***SI Appendix***, **Fig. S1*B***).

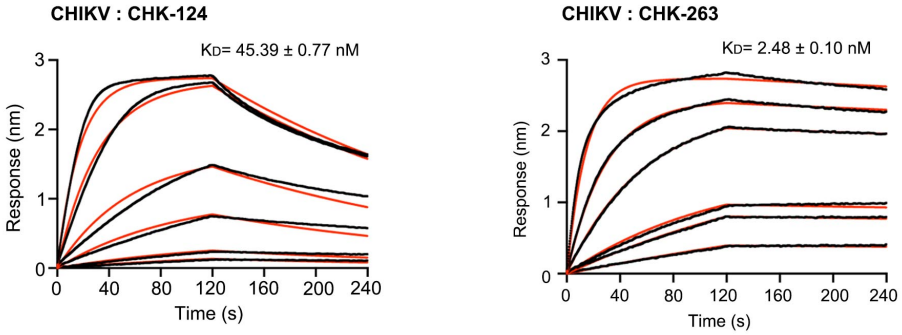

Fig. S10. Binding kinetics of CHK-124 Fab and CHK-263 Fab to CHIKV. The binding profile of CHK-124 (***left***) and CHK-263 (***right***) measured by biolayer interferometry. The CHIKV particles were captured on the biosensor with a human anti-CHIKV MAb and then dipped into wells containing CHK-124 or CHK-263 Fab. The Fab concentrations in the curves, from top to the bottom, are in a two-fold dilution starting from 500 nM. The Raw data curves are shown in black, and fitted curves are shown in red. The standard 1:1 binding model is applied to determine the binding affinity (K_D) of the Fab molecule to the CHIKV particle. Each graph represents one experiment from three independent experiments.

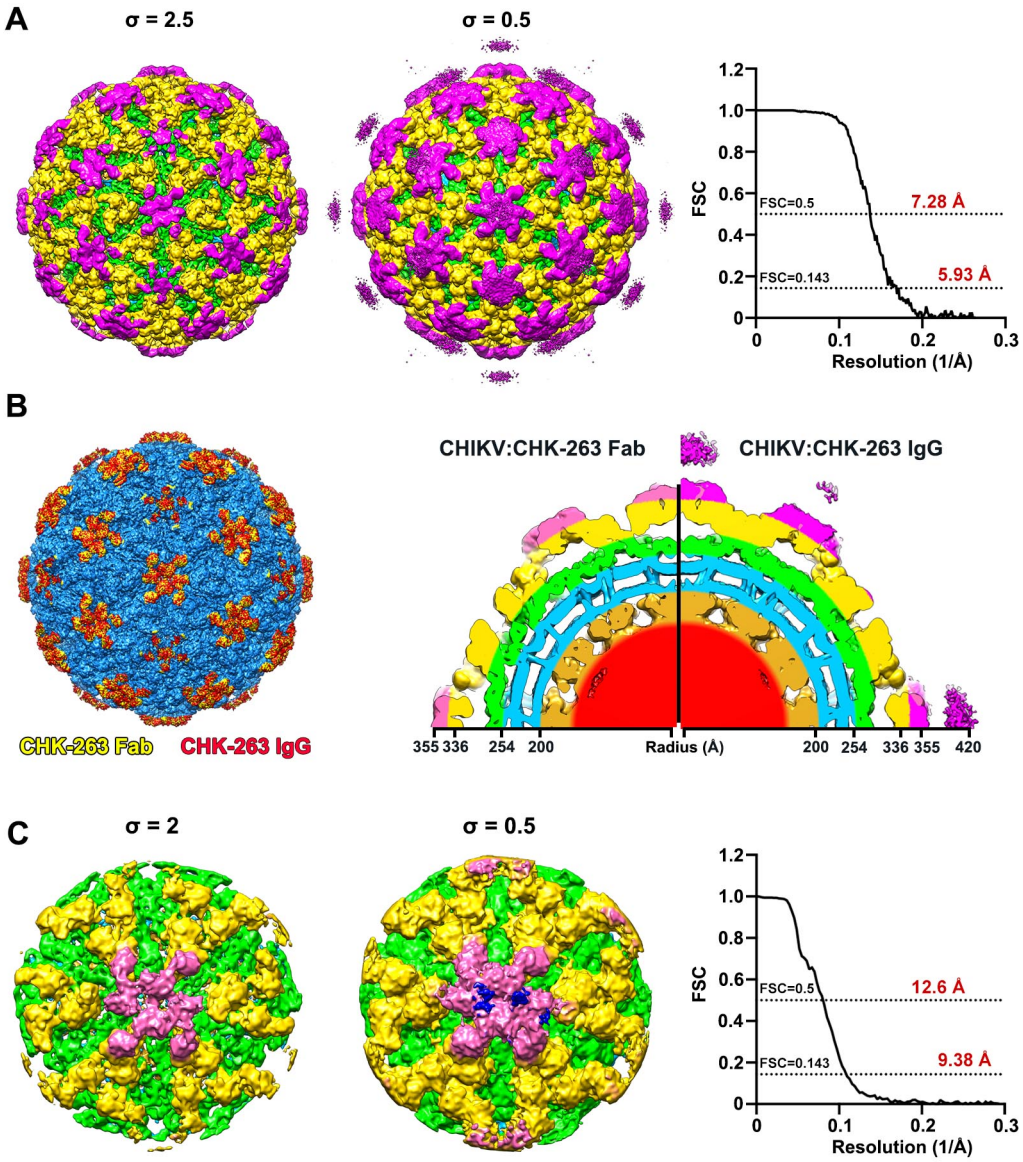

Fig. S11. Cryo-EM density maps of CHIKV:CHK-263 IgG complex structure. (***A***) The icosahedrally averaged cryo-EM map of the CHIKV:CHK-263 IgG complex was determined to 5.9-Å and displayed in different contour levels. In lower contour level, we observed weak densities which likely belonging to the Fc region around the 5- and 2-fold vertices. The right most panel showed FSC with the cut-off at 0.5 and 0.143. (***B***) Superposition of the cryo-EM maps of CHIKV complexed with IgG and Fab fragments of CHK-263. Left is the surface of the superimposed maps. Right shows their cross-sections. (***C***) Cryo-EM map of the asymmetric localized reconstruction of the 2-fold vertex sub-region of CHIKV:CHK-263 IgG complex determined to 9.4-Å and displayed in different contour levels. In lower contour level, we observed weak densities which likely belong to the Fc region around the 5- and 2-fold vertices. The right most panel showed FSC with the cut-off at 0.5 and 0.143. The hinge regions are colored in blue.

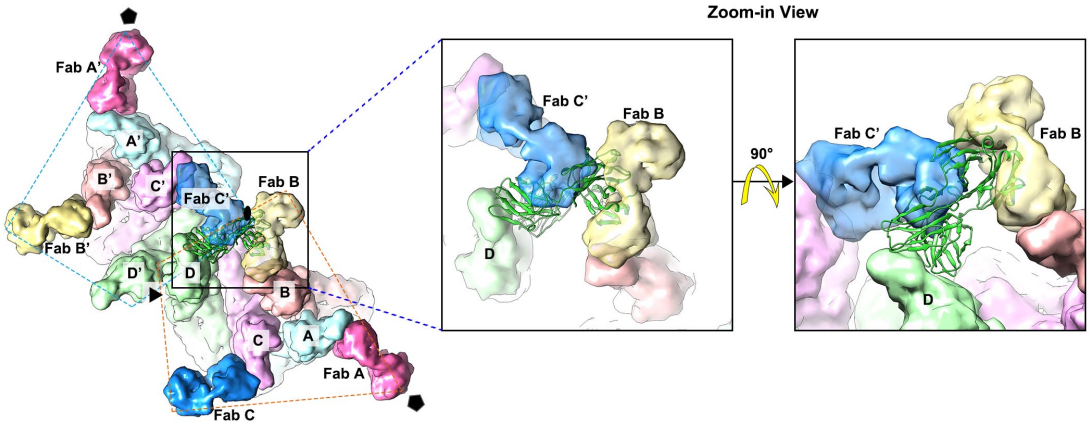

Fig. S12. The lack of CHK-263 Fab binding to E1-E2 mol D in an asymmetric unit may be caused by steric hindrance upon Fabs binding to neighboring E1:E2 molecules. Superposition of the E1-E2:CHK-263 Fab complex onto the unbound E1-E2 molecule D shows the Fab (green ribbon) will clash with neighboring Fab C' (blue surface) and B (tan surface) (black box). This suggests that when either Fab C' or B has bound to their respective E1-E2 heterodimers, Fab is not able to engage E1-E2 molecule D. Two asymmetric unit are shown by the blue and the orange dotted lines. Fab A-D and A'-D' correspond to the Fabs that bind at E1-E2 molecule A-D and A'-D' respectively. The bottom panel shows the enlarged top and side views of the clash of superimposed Fab D with the bound Fabs C' and B.

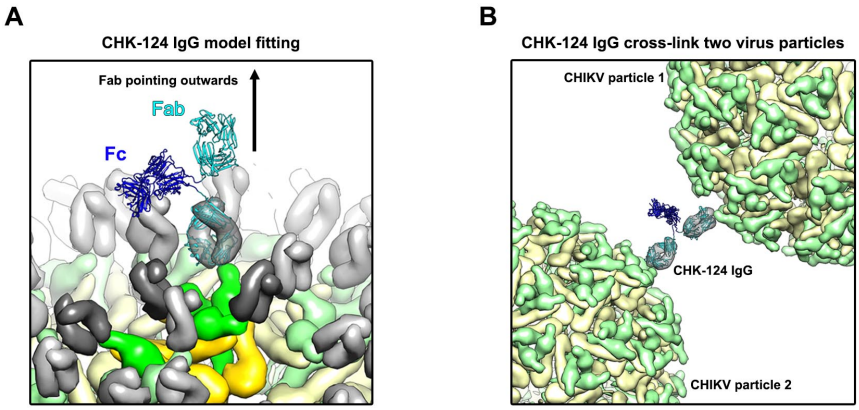

Fig. S13. Possible bivalent binding of the CHK-124 IgG onto the CHIKV particle surface showed CHK-124 IgG likely can cross-link different CHIKV particles. (***A***) Fitting of a Fab arm of the IgG crystal structure (PDB: 1IGT) into the CHIKV particle. The fitted IgG is shown as ribbon with its Fc and Fab fragments colored in blue and cyan, respectively. The black arrows next to the unbound Fab indicate that it is pointing outwards. (***B***) The two Fab arms of an IgG may bind two CHIKV-particles.

Table S1. Cryo-EM reconstruction, refinement and validation statistics

Protein Model		CHIKV + CHK-124	CHIKV + CHK-263	CHIKV + CHK-263 Fab (5-fold)	CHIKV + CHK-263 IgG	CHIKV + CHK-263 IgG (2-fold)
EMDB		30476	30477	30479	30478	30480
PDB code		7CVY	7CVZ	7CW2	7CW0	7CW3
CHIKV strain		CHIKV-Ross	CHIKV-East African			
3D Reconstruction						
# of Micrographs		3,851	5,777	-	2,780	-
# of particles picked		116,021	176,396	942,552	45,657	825,840
# of particles for final refinement		68,406	164,158	401,533	29,946	14,693
Symmetry imposed		I	I	C1	I	C1
Map sharpening B-factor ($Å^2$)		-265	-242	-236	-150	-150
Resolution $_{FSC=0.143}$ (Å)		5.2	4.7	4.5	5.9	9.4
Resolution $_{FSC=0.5}$ (Å)		6.5	5.5	5.7	7.3	12.6
Model Refinement (Cα backbone)						
# of chains		20	16	49	16	46
# of residues		5,768	4,894	15,993	4,894	17,462
MolProbity score		1.65	1.65	1.65	1.65	1.81
All-atom clash score		0	0	0	0	0.46
Rotamer outliers (%)		NA	NA	NA	NA	NA
Ramachandran Plot values	Favoured (%)	NA	NA	NA	NA	NA
	Allowed (%)	NA	NA	NA	NA	NA
	Outliers (%)	NA	NA	NA	NA	NA

R.M.S Deviations	Bond lengths (Å)	NA	NA	NA	NA	NA
	Bond angles	NA	NA	NA	NA	NA
Correlation Coefficient by protein (mean ± std)	E1	0.740 ± 0.025	0.684 ± 0.014	0.717 ± 0.026	0.737 ± 0.026	0.739 ± 0.024
	E2	0.722 ± 0.031	0.671 ± 0.024	0.704 ± 0.009	0.712 ± 0.023	0.723 ± 0.020
	Capsid	0.743 ± 0.017	0.651 ± 0.017	0.660 ± 0.032	0.656 ± 0.018	0.664
	Fab	0.298 ± 0.013	0.348 ± 0.056	0.342 ± 0.056	0.453 ± 0.082	0.742 ± 0.025

Table S2. Probable interacting residues between the CHK-124 Fab and the CHIKV E1, E2 proteins.

CHIKV envelope protein			CHK-124 Fab	
Segment		**Amino acid residue**	**H-chain**	**L-Chain**
E2	**184-189**	Q184	W31, R50, F105	Y91
		S185	Y30, W31, F99, Y100, G101, F102, D104, F105	
		G186	N29, Y30, F99, Y100,	
		N187	Y100, G101, F102	
		V188	F102	
		K189	F102, G103	T31, N32,
	214-221	D214	F102	T31, S50
		K215	F102	Y53
		V216	F102, G103	S50
		I217	F102	
		N218	Y100, G101, F102	
		N219	N29, Y30, Y100, G101	
		K221	N29	

Table S3. Probable interacting residues between the CHK-263 Fab and the CHIKV E1, E2 proteins.

CHIKV E protein			CHK-263 Fab	
Segment		**Amino acid residue**	**H-chain**	**L-Chain**
E2	**198-199**	R198		N92
		Y199		N32, N92
	206-218	S206	Y31	
		N207	S30, Y31, W32	
		E208	W32, L100	
		L210	N58	N92, W94
		T211	N58	
		T213	D54, D56	
		K215	Y51, D54, G55, D56	
		V216	Y51	
		I217	S30, Y51	
		N218	F28, S29, S30	
	232	H232		N92, S93
	245-250	N245		S30
		A246		S30, D31, S67
		E247		S28, S30, S67, G68, D70
		D250		Q27, S28, S30
E1	**61-63**	K61		S30, D31, S52, S67
		C63		Q53

SI References

1. P. Pal *et al.*, Development of a highly protective combination monoclonal antibody therapy against Chikungunya virus. *PLoS Pathog* **9**, e1003312 (2013).
2. A. Baer, K. Kehn-Hall, Viral concentration determination through plaque assays: using traditional and novel overlay systems. *J Vis Exp* 10.3791/52065, e52065 (2014).
3. T. Oliphant *et al.*, Antibody recognition and neutralization determinants on domains I and II of West Nile Virus envelope protein. *J Virol* **80**, 12149-12159 (2006).
4. J. M. Fox *et al.*, Broadly Neutralizing Alphavirus Antibodies Bind an Epitope on E2 and Inhibit Entry and Egress. *Cell* **163**, 1095-1107 (2015).
5. G. Fibriansah *et al.*, A highly potent human antibody neutralizes dengue virus serotype 3 by binding across three surface proteins. *Nat Commun* **6**, 6341 (2015).
6. W. Akahata *et al.*, A virus-like particle vaccine for epidemic Chikungunya virus protects nonhuman primates against infection. *Nat Med* **16**, 334-338 (2010).
7. J. M. Smit, R. Bittman, J. Wilschut, Low-pH-Dependent Fusion of Sindbis Virus with Receptor-Free Cholesterol- and Sphingolipid-Containing Liposomes. *Journal of Virology* **73**, 8476-8484 (1999).
8. B. Carragher *et al.*, Leginon: an automated system for acquisition of images from vitreous ice specimens. *J Struct Biol* **132**, 33-45 (2000).
9. X. Li, S. Zheng, D. A. Agard, Y. Cheng, Asynchronous data acquisition and on-the-fly analysis of dose fractionated cryoEM images by UCSFImage. *Journal of Structural Biology* **192**, 174-178 (2015).
10. T. Grant, A. Rohou, N. Grigorieff, cisTEM, user-friendly software for single-particle image processing. *eLife* **7** (2018).
11. K. Zhang, Gctf: Real-time CTF determination and correction. *Journal of Structural Biology* **193**, 1-12 (2016).
12. S. H. Scheres, RELION: implementation of a Bayesian approach to cryo-EM structure determination. *J Struct Biol* **180**, 519-530 (2012).
13. J. Zivanov *et al.*, New tools for automated high-resolution cryo-EM structure determination in RELION-3. *Elife* **7** (2018).
14. S. L. Ilca *et al.*, Localized reconstruction of subunits from electron cryomicroscopy images of macromolecular complexes. *Nat Commun* **6**, 8843 (2015).
15. S. H. W. Scheres, Processing of Structurally Heterogeneous Cryo-EM Data in RELION. **579**, 125-157 (2016).
16. P. V. Afonine *et al.*, Real-space refinement in PHENIX for cryo-EM and crystallography. *Acta Crystallogr D Struct Biol* **74**, 531-544 (2018).
17. P. Emsley, K. Cowtan, Coot: model-building tools for molecular graphics. *Acta Crystallographica Section D* **60**, 2126-2132 (2004).
18. V. B. Chen *et al.*, MolProbity: all-atom structure validation for macromolecular crystallography. *Acta Crystallogr D Biol Crystallogr* **66**, 12-21 (2010).
19. N. A. Baker, D. Sept, S. Joseph, M. J. Holst, J. A. McCammon, Electrostatics of nanosystems: application to microtubules and the ribosome. *Proc Natl Acad Sci U S A* **98**, 10037-10041 (2001).
20. T. J. Dolinsky, J. E. Nielsen, J. A. McCammon, N. A. Baker, PDB2PQR: an automated pipeline for the setup of Poisson-Boltzmann electrostatics calculations. *Nucleic Acids Res* **32**, W665-667 (2004).

21. H. Li, A. D. Robertson, J. H. Jensen, Very fast empirical prediction and rationalization of protein pKa values. *Proteins* **61**, 704-721 (2005).
22. C. R. Søndergaard, M. H. M. Olsson, M. Rostkowski, J. H. Jensen, Improved Treatment of Ligands and Coupling Effects in Empirical Calculation and Rationalization of pKa Values. *Journal of Chemical Theory and Computation* **7**, 2284-2295 (2011).
23. J. E. Voss *et al.*, Glycoprotein organization of Chikungunya virus particles revealed by X-ray crystallography. *Nature* **468**, 709-712 (2010).